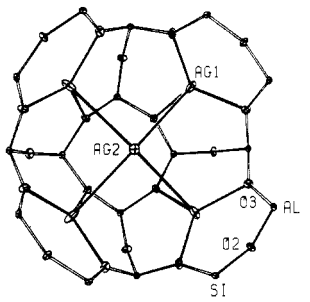

Figure 2. Possible isolated Ag atom coordinated to four Ag^+ ions to give $(Ag_5)^{4+}$, symmetry *4mm*. Each Ag^+ ion coordinates to the three O(3) oxygens of a 6-ring.

seen in other structures such as $Tl_{6.5}Ag_{5.5}$-A dehydrated at 440 °C[23] and Ag_{12}-A treated first with H_2 and then with O_2, both at 330 °C.[22]

It may be that a neutral hexasilver cluster has formed in one-sixth of the sodalite units.[1,2] It is also possible that an isolated atom exists in each sodalite unit, coordinated to at least 2.6 Ag^+ ions. This is the number of the original 6.6 Ag^+ ions remaining if the maximum number of Ag^+ ions per sodalite unit (4) position themselves far from the Ag^0 atom. It appears far more reasonable that the maximum number of Ag^+ ions would position themselves near the Ag^0 atom to give $(Ag_5)^{4+}$, symmetry *4mm* (see Figure 2). Ag_6 and $(Ag_5)^{4+}$, then, seem to be the two most reasonable interpretations of the crystallographic result. Other clusters involving metal-metal bonds such as $(Ag_8)^{6+}$ (the result of two $(Ag_5)^{4+}$ units sharing two Ag^+ ions) or $(Ag_{12})^{8+}$ (the result of four $(Ag_5)^{4+}$ units sharing all eight Ag^+ ions) remain possible but seem less likely and too numerous to discuss.

The cation which has been reduced is the one which is most easily reduced, Ag^+, and the cation site which is no longer occupied is the least favorable, the one opposite a 4-ring in the large cavity. This position is the least satisfactory because the approach of the Ag^+ ion to framework oxygens has been the longest (possibly virtual) and the most one-sided in previous studies.[1,2,30]

The ionic radius[28] of Ag^+, 1.26 Å, is much larger than that of Na^+, 0.97 Å. From a consideration of ionic radii only, one would expect the larger Ag^+ ions to associate with the larger rings, the 8-rings. However, Ag^+ ions are all found in 6-ring sites as predicted by the calculations of Nitta et al.[14] and as demonstrated less directly by the experiments of Schöller et al.[12]

Ag_{12}-A dehydrated at 350 °C has three water molecules in each sodalite unit, together with three Ag^+ ions and no reduced silver atoms.[30] Ag_{12}-A dehydrated at temperatures ≥ 400 °C for about 2 days has no residual water and contains reduced silver atoms.[1,2] In this work, we observe 370 °C is a sufficiently high temperature to have brought about the complete dehydration and the partial reduction of Ag^+ in $Ag_{7.6}Na_{4.4}$-A. Perhaps the formation of the silver atom and the loss of the last water molecule(s) occur together as a concerted process.

A comparison of this structure with that of dehydrated (at 350 °C) Ag_6Na_6-A treated with H_2[3] and with dehydrated (at 350 °C) $Ag_{4.6}Na_{7.4}$-A treated with H_2[5] indicates that all of the reduced silver atoms and 8-ring Ag^+ ions in those structures were Ag^+ ions in 6-rings before H_2 was added, except for one silver atom per unit cell which may have formed during dehydration. Some 6-ring Ag^+ ions moved to 8-ring sites to coordinate to silver atoms or clusters.

Acknowledgment. This work was supported by the National Science Foundation (NSF-INT-83-16234) and by the Korean Science and Engineering Foundation.

Supplementary Material Available: Table of calculated and observed structure factors (2 pages). Ordering information is given on any current masthead page.

(30) Kim, Y.; Seff, K. *J. Phys. Chem.* **1978**, *82*, 1071-1077.

Meaning and Structure of Amphiphilic Phases: Inferences from Video-Enhanced Microscopy and Cryotransmission Electron Microscopy

D. D. Miller, J. R. Bellare, D. F. Evans,*

Department of Chemical Engineering and Materials Science, University of Minnesota, Minneapolis, Minnesota 55455

Y. Talmon,

Department of Chemical Engineering, Technion—Israel Institute of Technology, Haifa 32000, Israel

and B. W. Ninham

Department of Applied Mathematics, Research School of Physical Sciences, Institute of Advanced Studies, Australian National University, Canberra A.C.T., 2601 Australia *(Received: June 9, 1986; In Final Form: September 8, 1986)*

This paper attempts to come to grips with a major issue confronting association colloid science. It does so by illustrating some surprising features of aggregates of simple amphiphiles as revealed by two powerful complementary tools, video-enhanced microscopy (VEM) and cryotransmission electron microscopy (cryo-TEM), both of which allow direct visualization. The natures of these aggregates challenge existing theories and show up limitations of some other noninvasive, though indirect, techniques. The problem of the meaning of amphiphilic phases and their microstructure is discussed and the necessity for a different descriptive language emphasized.

1. Introduction

1.1. Problem. No one schooled in classical thermodynamics has any doubts on the existence of phases. The world of equilibrium homogeneous and heterogeneous substances is made up of phases—in the thermodynamic limit. It is a matter of definition. For example, the phase diagrams of (a) a nonionic single-chained surfactant ($C_{12}EO_6$) and (b) a double-chained cationic (dido-

0022-3654/87/2091-0674$01.50/0

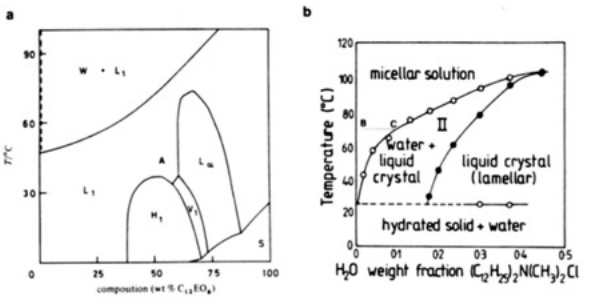

Figure 1. (a) Phase diagram of $C_{12}EO_6$ (from ref 1). L_1 = isotropic phase, W = water + surfactant monomer, H_1 = hexagonal phase, V_1 = bicontinuous cubic phase, L_α = lamellar phase. (b) Phase diagram of didodecyldimethylammonium chloride (from ref 2).

decyldimethylammonium chloride) in water are illustrated in Figure 1. Solutions of surfactants are assumed to be made up of micellar (spheres), hexagonal (cylinders), and lamellar (planes) phases in a kind of Pythagorean imperative in which the inferences of visual inspection or simple measurements like viscosity are reconfirmed by a variety of noninvasive, though indirect, techniques.

The nonuniqueness of scattering theory and the necessary model dependence required for the interpretation of NMR and X-ray, neutron, or quasi-elastic light scattering, however, mean that we see those structures that our models demand that we see. The theorem that any continuous, differentiable function can be approximated to arbitrary accuracy by a polynomial of sufficiently high order (or a Padé approximant) has an interesting consequence. In the context of scattering theory, it means that the form factor $S(q)$ must be known for *all* values of the momentum-transfer variable q. Even then the deficiencies of numerical analysis will impose limitations. It is possible to fit scattering data from an isotropic L_2 phase (oil, water, surfactant) to any, of say, mixtures of spheres, cylinders, or minimal curvature bicontinuous structures to arbitrary accuracy, even when the system under study is otherwise known to be a chaotic bicontinuous medium of average *constant* Gaussian curvature. There exists no mathematical theory yet provided by geometric topology to describe or elucidate the generality of such conceivable structures. It is not even known if the class of regular commensurate structures of fixed curvature is finite or infinite. Again, self-similar structures, which scale over many orders of magnitude, of a kind to be illustrated below, have an underlying mathematical description in terms of continuous nondifferentiable functions.

An additional problem is that phase boundaries are frequently not sharply defined for amphiphilic systems and are often chosen by some arbitrary experimental criterion.[2,3] Furthermore, an in-principle well-defined X-ray pattern from liposomal structures in an isotropic background will be subject to intensity detection limitations. The issue of ill-defined phases is severe and cannot be ignored if we are ever to interpret the bewildering variety of pictures with which cell biology confronts us.

Two examples might serve to make our point explicit.

(1) For a dilute system of near spherical micelles above the critical micelle concentration, we have no great difficulty in defining the structure and size or what is meant by a phase. But on addition of salt or increase in concentration in ionics or increase of temperature or concentration in nonionics, the micelles grow and become sometimes polydisperse. They grow through shapes crudely categorized as disks, oblates, spheroids, or rods. The matter has occasioned great debates, resolved by the weight of opinion in favor of one or the other structure. It will be recalled that Hartley's original spherical micelle model was heresy for a long time, since dogma asserted that micelles had to be bits of lamellae. In such an isotropic solution, is the system at point A of Figure 1a to be considered as one-phase micellar or a multicomponent mixture of micellar, disordered precubic disks, near hexagonal and/or lamellar phases? Our point A is certainly a point of indecision for any anthropomorphic surfactant monomer. The sequence of different shapes exhibited by phospholipid and other membrane mimetic vesicles throws that problem into stark relief.[4]

(2) Again, consider the evolution of microstructure along the line BC of Figure 1b. (Figure 1b is the phase diagram for didodecyldimethylammonium chloride but is representative of many double-chained surfactants such as the dialkyl halides and the so-called Texas No. 1 [sodium 8-phenyl-*n*-hexadecyl-*p*-sulfonate] to be discussed later.) At low concentrations the isotropic "micellar" solution comprises a mixture of single-walled vesicles and micelles as will be shown below. With increasing surfactant concentration (along BC), the fraction of surfactant in micelles increases and the vesicles *decrease* in size, until at the boundary C a proportion of larger aggregates begin to appear. With very

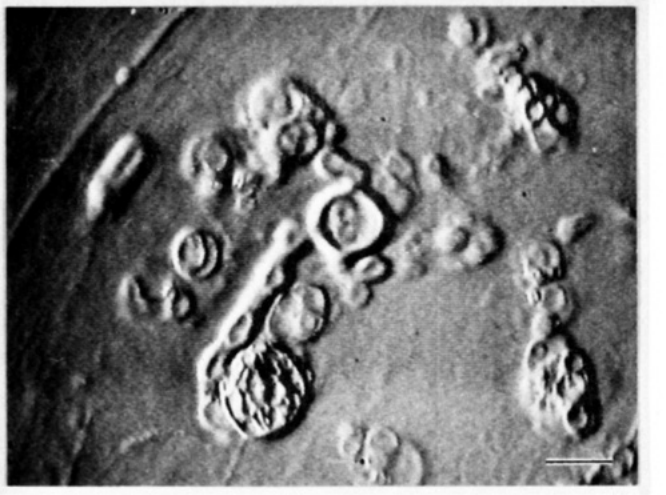

Figure 2. VEM micrograph of typical structures formed upon neutralization of 10^{-3} M didodecyldimethylammonium hydroxide by HBr with free convection mixing. Bar = 10 μm.

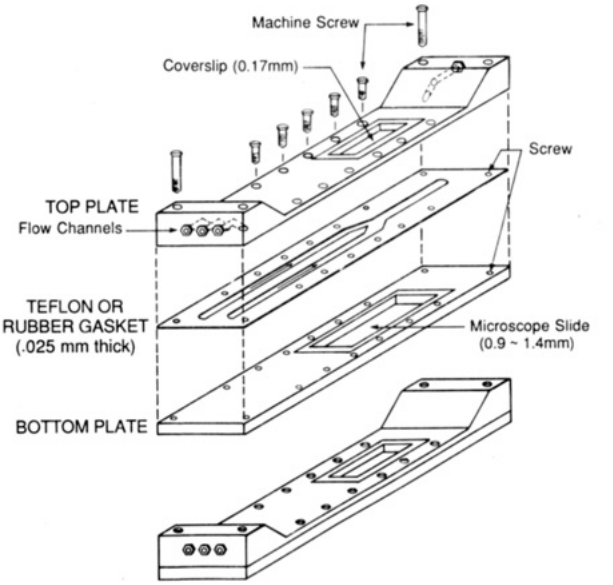

Figure 3. Microscope flow cell used to determine the effect of flow and to examine chemically induced transformations with VEM. In the configuration shown, the center of the three ports would be closed while solution and reagent would enter the outer ports, flow down the channels cut in the gasket, and join at the channel intersection, forming a sharp interface.

(1) Mitchell, D. J.; Tiddy, G. J. T.; Waring, L.; Bostock, T.; McDonald, M. P. *J. Chem. Soc., Faraday Trans. 1* **1983**, *79*, 975.
(2) Kunieda, H.; Shinoda, K. J. *Phys. Chem.* **1978**, *82*, 1710.
(3) Franses, E. I., et al. *ACS Symp. Ser.* **1979**, *91*, 35.

(4) Sackman, E.; Duwe, H. P.; Engelhardt, H. *Faraday Discuss. Chem. Soc.*, in press.

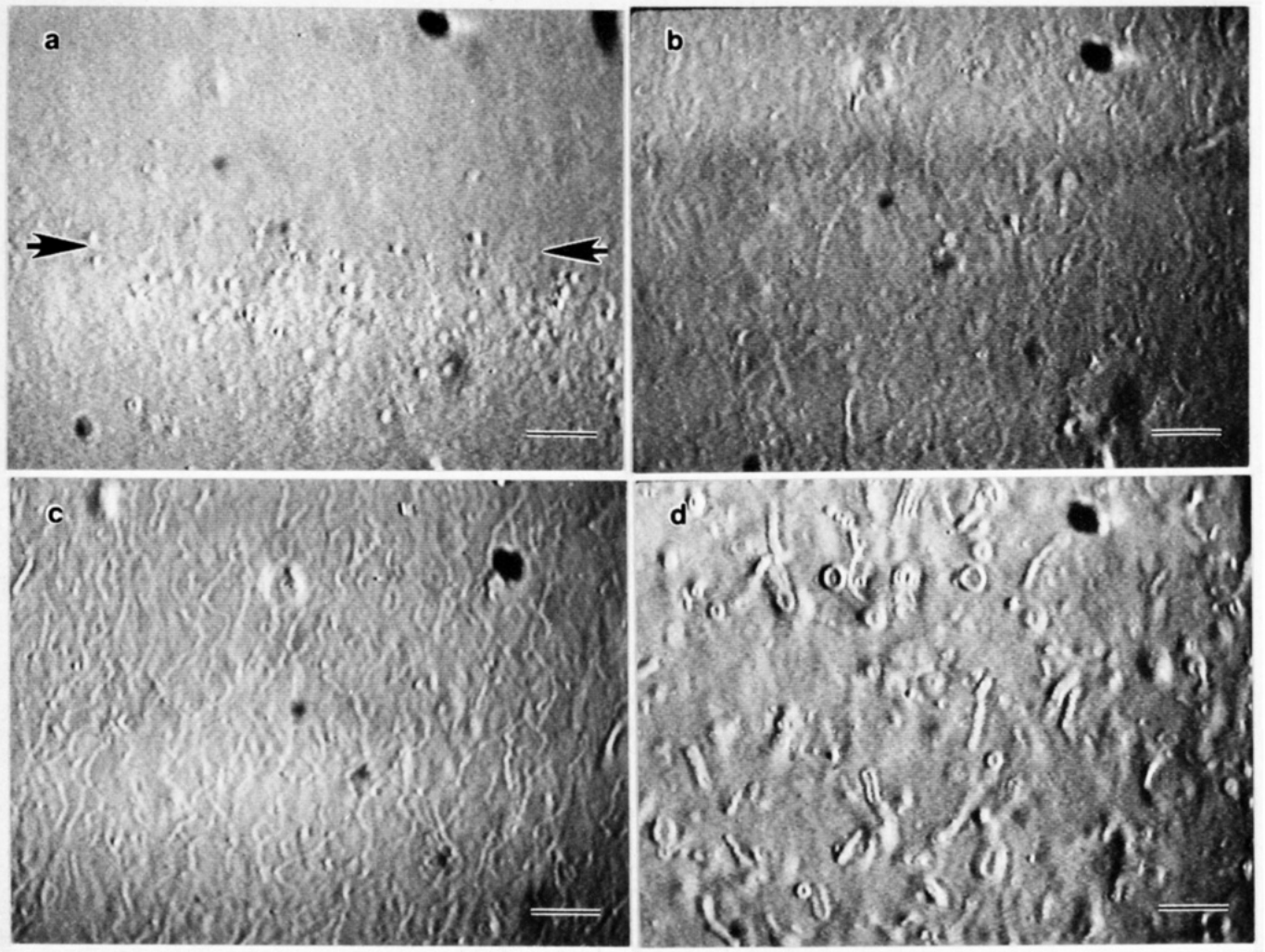

Figure 4. Sequence of structures formed upon neutralization of 10^{-3} M didodecyldimethylammonium hydroxide by HBr in the flow cell and examined with VEM (Figure 3). Bar = 10 μm. (a) Zero time: $2C_{12}N2C_1OH$–HBr interface formed by initial left to right flow is indicated by arrows. Clear field is acid solution at top. Growing vesicles are in the lower portion of the micrograph. (b) One minute after the flow stops: particles grow and "worms" begin to form. (c) Ten minutes later: solution filled with worms with preferential orientation in the direction of the acid–base concentration gradient. (d) Forty-five minutes later: worms have transformed into spherical particles which slowly grow.

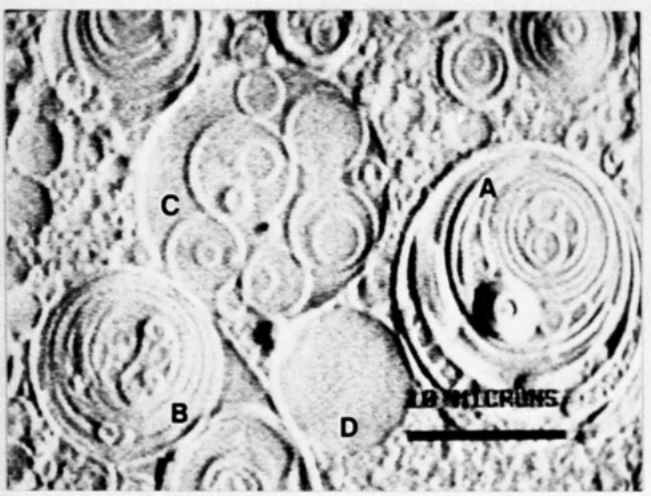

Figure 5. VEM micrograph of 1.7% SHBS. Bar = 10 μm. (A, B) Liposomes (birefringent under crossed polars). (C) Large vesicle containing entrapped smaller vesicles. (D) Vesicle with a "dust-storm" appearance in real time, indicating that it is filled with small, unresolvable particles.

large structures, well into the "two-phase" region, we have no difficulty in characterizing those aggregates which give well-defined X-ray scattering spacing as liposomes or lamellar phase. But are the small single- or several-walled vesicles that coexist with these larger liposomes to be counted as lamellar phase or micellar? Or none of the above?

1.2. Tyranny of Theory. The canonical description of multicomponent systems embraced by thermodynamics says nothing of microstructure. The justification through statistical mechanics of the link between molecular properties and macroscopic condensed matter physics nowhere deals with the shape and size of aggregates of solute molecules. Nor in the transition from microscopic to infinite systems does statistical mechanics deal properly with polydispersity. Even the writing down of a partition function which simultaneously averages over *shapes* and energies of physically associated amphiphiles is not possible at this time. Hence, attempts to construct solution theories for the small system thermodynamics required for association colloids have been subject to severe constraints. Analytically accessible microstructures (spheres, cylinders, planes) to which statistical mechanics adjoins some theory of interactions have allowed some progress to be made in understanding amphiphilic aggregation.[5-7] These theories are abstracted, e.g., from the primitive model of electrolytes and double-layer theory for ionics.

But these theories tend to take on a reality beyond the limits of their applicability. If theory deals only with spheres, rods, planes, and bicontinuous surfaces of minimal curvature, and if

(5) Gunnason, G.; Jönsson, B.; Wennerström, H. *J. Phys. Chem.* **1980**, *84*, 3114.
(6) Evans, D. F.; Mitchell, D. J.; Ninham, B. W. *J. Phys. Chem.* **1984**, *88*, 6344.
(7) Jönsson, B.; Wennerström, H. *J. Phys. Chem.*, in press.

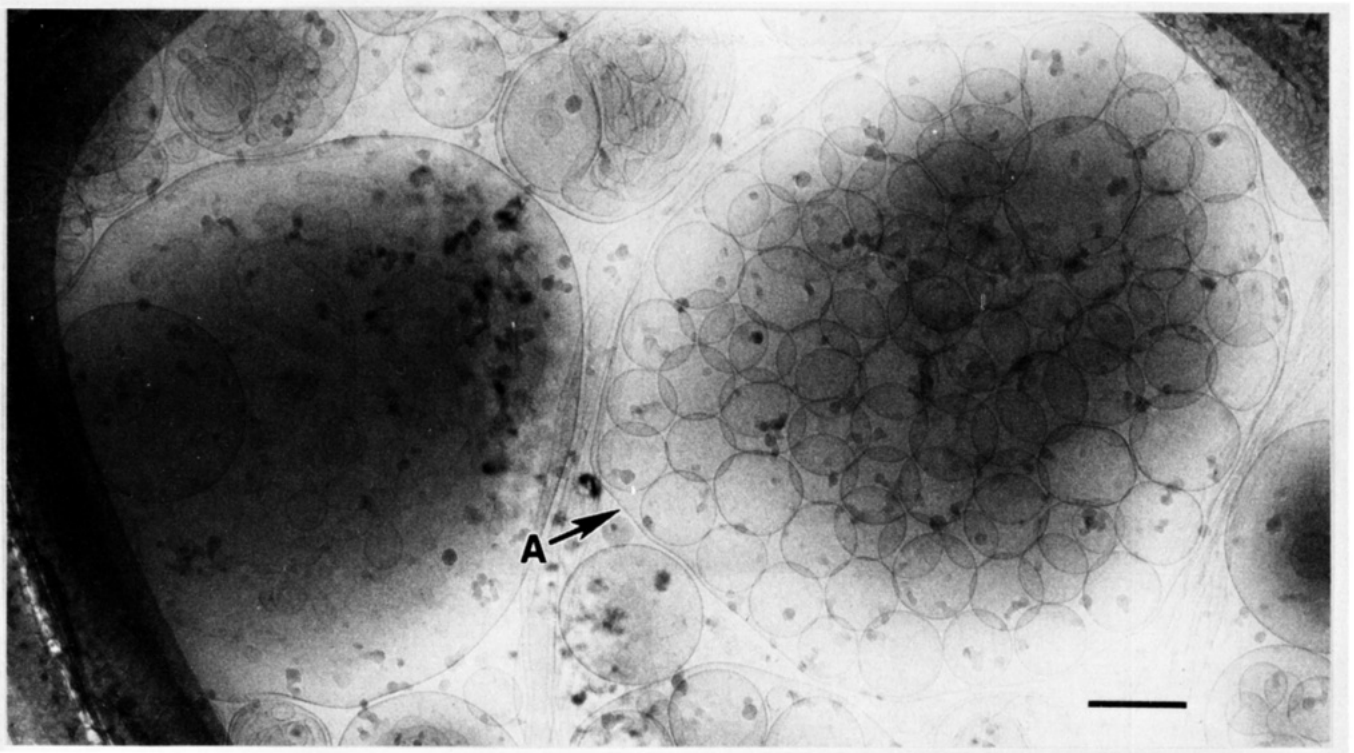

Figure 6. Vitrified hydrated unstained (VHU) cryo-TEM picture of a 1.7 wt % SHBS sample prepared with CEVS. Note large (1.75 μm) single-walled vesicle (A) encapsulating many smaller vesicles. Bar = 0.25 μm.

experiment uses theory as it must for interpretation, then theory is likely to be confirmed, and real subtleties will be masked. In writing down the free energy of an aggregate of assumed size and shape (sphere, cylinder) to be minimized to determine the "optimal" aggregate, we extend thermodynamics to small systems. We assume a form for the chemical potential of a monomer in an aggregate like

$$\mu = \mu_B + \mu_S + \mu_{interaction} \quad (1)$$

Here μ_B is an assumed free energy of transfer of a monomer to the hydrophobic core of an aggregate of aggregation number N. To lowest order, the surface contribution μ_S is proportional to $N^{2/3}$, and $\mu_{interaction}$ is of higher order still. These are shape and model-dependent contributions to μ which are functions of head group area and concentration. Extensions of this simplest level of theory beyond leading curvature corrections become intractable. This is because fluctuations in curvature energies can be of the same order as interaction terms, and of the same order as the approximation injected by (arbitrary) choices of concentration units.

Such approximations are acceptable in some regimes, e.g., noninteracting monodisperse micelles or ionic micelles with high ion binding parameters so that interactions[8] are muted. But the approximations are not generally valid since eq 1 may not be appropriate when the variable chosen for minimization (like head group area) is allowed to deviate from its optimal value. Thus, for a lamellar phase, in any variation from optimal head group area, the pressure becomes anisotropic and Gibbs free energy is undefined.

Interactions also pose a problem. The intuition concerning interactions between aggregates involves an extrapolation and extension from the macroscopic to the microscopic. Thus, the apparent agreement between direct measurements of double-layer forces[9] between molecularly smooth surfaces and predictions of the Poisson–Boltzmann equation with or without decorations are used to argue that ionic micelle–micelle interactions can be modeled by the same notions.[5,7] But the first involves one adjustable parameter, the degree of surface dissociation, and the second another, the size of a hydrated counterion in the primitive model. The agreement is illusionary, and all short-range surface forces due to water structure[10] ultimately responsible for aggregation are disguised in hidden parameters. Continuum van der Waals theories for attractive forces are asymptotic, hold only at large distances, and cannot be generally valid.[11] To illustrate this, consider the measured force between two electrically neutral fully hydrophobic surfaces in water.[12] The force is long range, with an exponential decay length of 1 nm. It is 10–100 times larger than the continuum prediction of Lifshitz theory and merges into that asymptotic result only at around 15 nm. Yet the force between two small hydrophobic molecules is surely short range and essentially zero beyond one or two molecules. In the intermediate micellar size range, the interactions between two micelles involve rearrangement of head groups and consequent exposure of hydrophobic surface areas which can be large on a molecular scale (25–100 Å^2) in ways not understood or accessible. The careful distinction always made between emulsions (metastable) and microemulsions (equilibrium) is an example of this problem of the range of attractive forces in small systems. Obviously there is no distinction, and the distinction needs to be made only if we insist that macroscopic thermodynamics maps over directly to small systems.

All this is not to say that present theories are not sometimes acceptable, or even quantitatively correct—in a limited temperature range. But the difficulties we have tried to pinpoint do suggest that the usual characterization of phases in surfactant systems as micellar, isotropic viscous, etc., are limited. An as yet vaguely circumscribed consensus is emerging that the canonical variables of thermodynamics do not form the best basis for a complete description of surfactant aggregation. A broader description has to relate directly observable microstructures to net curvature, size, and long-range interactions (concentration and/or ionic strength).

2. Techniques

We now describe two complementary techniques which allow

(8) Ninham, B. W.; Evans, D. F. *Faraday Discuss. Chem. Soc.*, in press.
(9) Pashley, R. M.; McGuiggan, P. M.; Ninham, B. W.; Brady, J.; Evans, D. F. *J. Phys. Chem.* **1986**, *90*, 1637.
(10) Wojcik, M. J.; Rice, S. A. *J. Chem. Phys.* **1986**, *84*, 3042.
(11) Mahanty, J.; Ninham, B. W. *Dispersion Forces*; Academic: New York, 1974.
(12) Pashley, R. M.; McGuiggan, P. M.; Ninham, B. W.; Evans, D. F. *Science (Washington, D.C.)* **1985**, *229*, 1088.

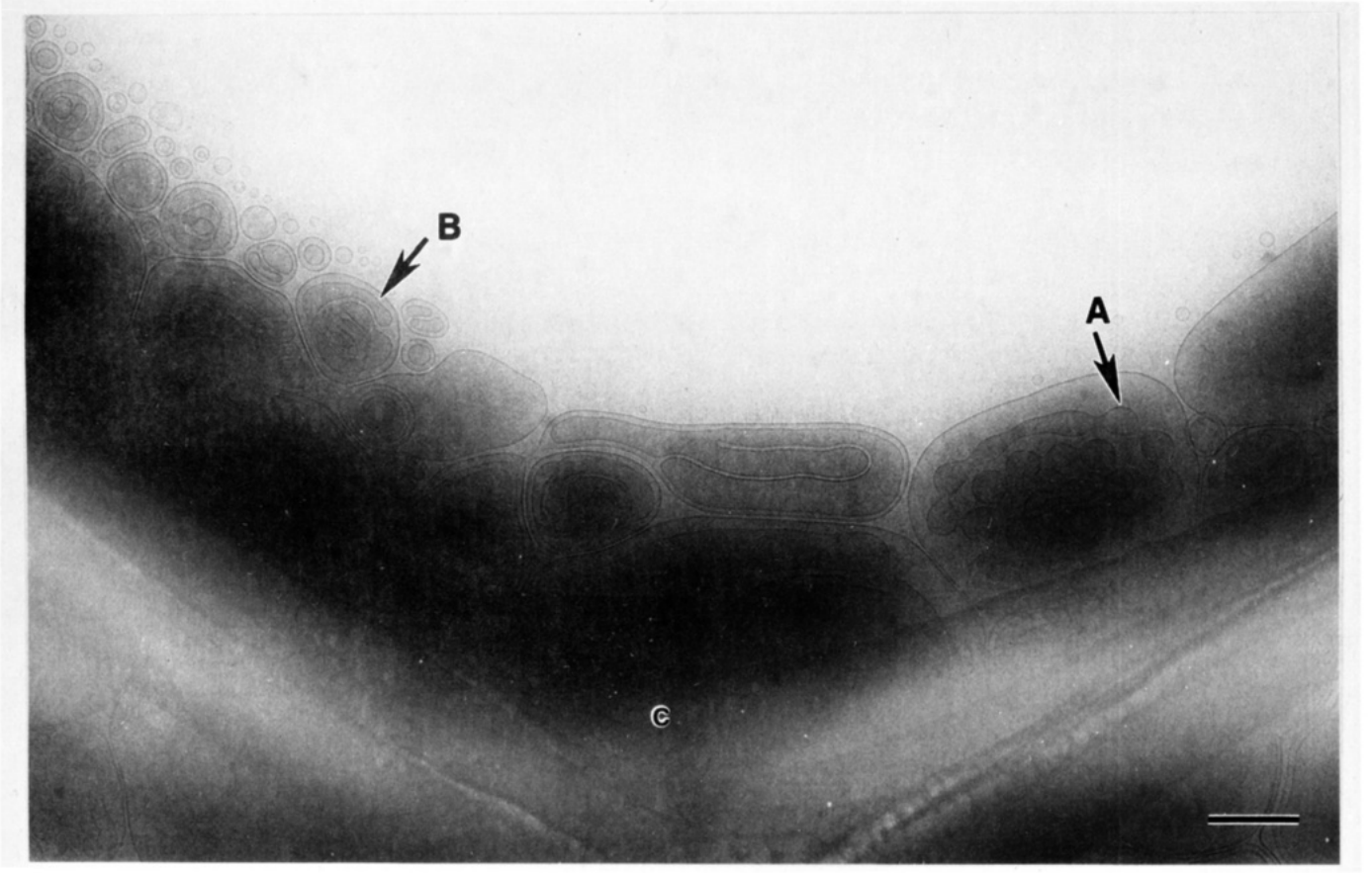

Figure 7. Electron micrograph of 1.7% SHBS showing vesicle-encapsulated microtubules. (A) Microtubule in the process of budding off to form small vesicles; (B) coiled microtubule. Bar = 0.25 μM.

direct visualization of microstructure within a single "phase" in ways not previously possible. This makes specific the problems outlined above.

2.1. Cryotransmission Electron Microscopy (Cryo-TEM). Transmission electron microscopy (TEM) is the natural technique of choice to study surfactant aggregates because it provides high-resolution *direct images*. But TEM specimens must be compatible with the high vacuum in the microscope ($<10^{-6}$ Torr) and must be thin (<0.25 μm). Also all motion on the supramolecular scale must be arrested to prevent image blurring. These factors have greatly limited the applicability of TEM in colloid science because of inadequate specimen preparation techniques that have not been able to preserve the original system microstructure in the final TEM specimen. Failure of these techniques has been the result of either change of concentration by drying, addition of a stain or fixation agent, or freezing the specimen at rates too slow to prevent microstructural rearrangement prior to complete fixation. Talmon and co-workers have described the sources of artifacts in the traditional TEM specimen preparation techniques, many of them borrowed from the biological sciences, as applied to the research of surfactant systems.[13-16]

For quite some time it has been established that thermal fixation, i.e., ultrafast cooling, is superior to drying and chemical fixation that involves an addition of an alien compound to the system. Successful examples of application of these so-called cryoelectron microscopy techniques were mainly limited to systems of low solubility surfactants where solute rearrangement during specimen preparation was negligible. These include applications of freeze fracture techniques,[17,18] where a replica of the fractured frozen specimen is examined in the TEM, and of direct imaging ("cold-stage") techniques, where the frozen specimen itself is examined in the TEM.[19-21]

When cooling rates are fast enough, water in the specimen solidifies without crystallization, forming a vitreous ice ($\mathbf{I}_v$) matrix. In such a specimen, phase separation and solute segregation during thermal fixation are avoided. Dubochet and co-workers[22] were the first to show a practical technique for vitrifying thin TEM specimens. Talmon[23] and Bellare et al.[24] have shown the potential of this technique for elucidating the microstructure of surfactant systems. In addition to preserving the original microstructure of the systems, vitrified specimens exhibit better contrast between surfactant aggregates and the $\mathbf{I}_v$ matrix, contrast which is not complicated by the presence of a hexagonal ice ($\mathbf{I}_h$) matrix (in which the images of inclusions (e.g., vesicles) do not reveal their inner structure[20]). This is the reason that in our earlier work[21] we could not determine whether the didodecyldimethylammonium hydroxide vesicles were unilamellar or multilamellar. As can be seen below, transmission electron micrographs of vitrified specimens show very clearly the inner structure of surfactant aggregates. In fact this has made the present study possible. An additional advantage of working with vitrified rather than crystallized specimens is that the former are much less susceptible to electron beam radiation damage than the latter.[25]

(13) Talmon, Y. *J. Colloid Interface Sci.* **1983**, *93*, 366.
(14) Kilpatrick, P. K.; Miller, W. G.; Talmon, Y. *J. Colloid Interface Sci.* **1985**, *107*, 146.
(15) Kilpatrick, P. K.; Miller, W. G.; Talmon, Y. Paper presented at the Proceedings of the 5th International Symposium on Surfactant in Solution, Bordeaux, July 1984.
(16) Talmon, Y., ref 15.
(17) Bachmann, L.; Dasch, W.; Kutter, P. *Ber. Bunsenges. Phys. Chem.* **1981**, *85*, 883.
(18) Zasadzinski, J. A.; Scriven, L. E.; Davis, H. T. *Philos. Mag. A* **1985**, *A51*, 287.
(19) Talmon, Y.; Davis, H. T.; Scriven, L. E.; Thomas, E. L. *Rev. Sci. Instrum.* **1979**, *50*, 698.
(20) Falls, A. H.; Davis, H. T.; Scriven, L. E.; Talmon, Y. *Biochim. Biophys. Acta* **1982**, *693*, 364.
(21) Talmon, Y.; Evans, D. F.; Ninham, B. W. *Science (Washington, D.C.)* **1983**, *221*, 1047.
(22) Adrian, M.; Dubochet, J.; Lepault, J.; McDowell, A. W. *Nature (London)* **1984**, *308*, 32.
(23) Talmon. Y. *Colloids Surf.*, in press.
(24) Bellare, J. R.; Davis, H. T.; Scriven, L. E.; Talmon, Y. *J. Colloid Interface Sci.* (in preparation).

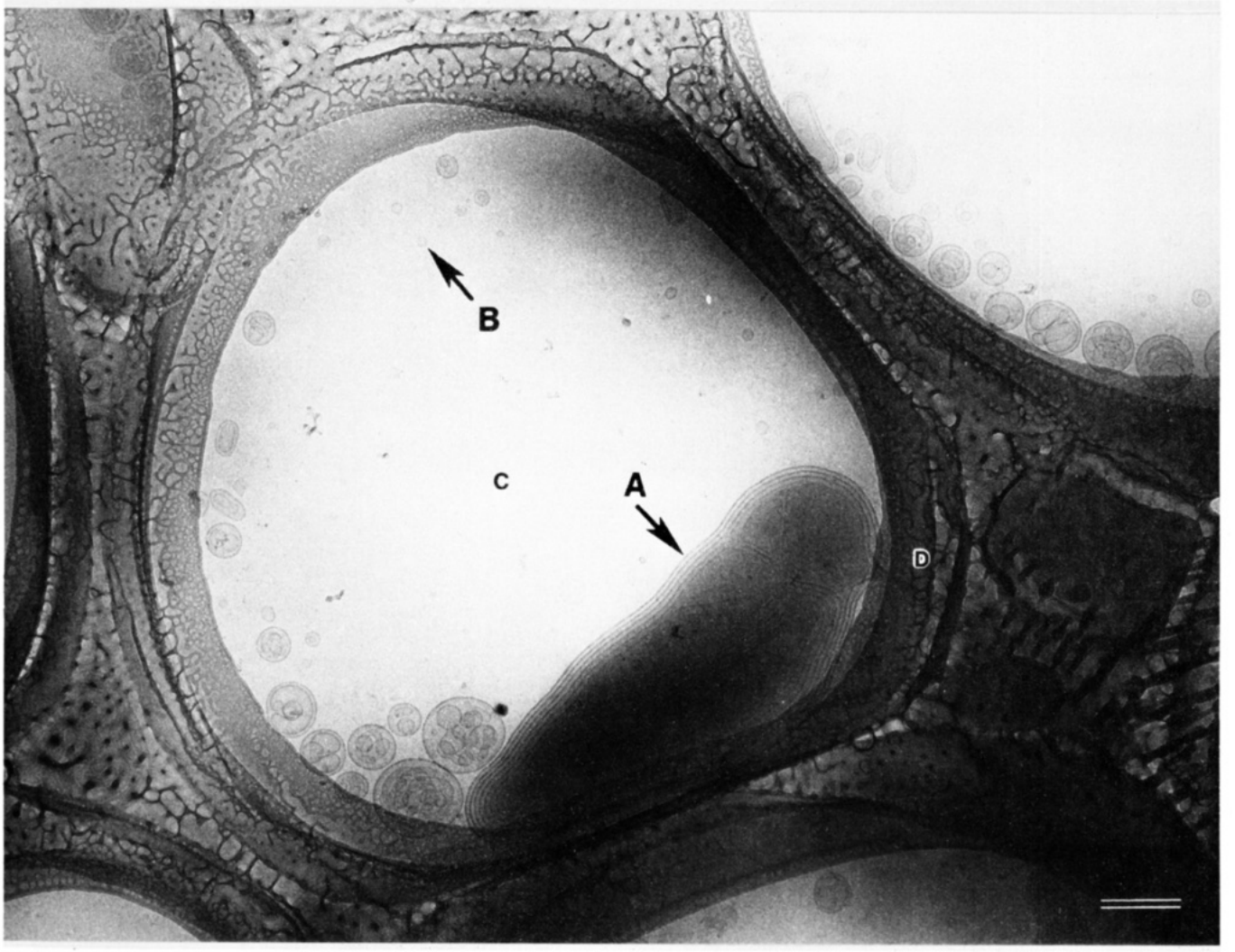

Figure 8. Vitrified solution of 1.7% SHBS showing liposome with closely spaced bilayers (A) and small (0.01 μm) vesicles (B) in vitreous water (C) spanning holes in carbon film (D). Bar = 0.25 μm.

Preparation of thin vitrified specimens of aqueous dispersions is relatively simple:[22,23] a drop of the liquid is applied onto a holey, carbon film covered TEM grid held by tweezers and mounted in a specially designed guillotine-type plunger. Most of the liquid is blotted away by pressing a filter paper to the grid, leaving behind thin liquid films spanning the holes in the carbon film. The grid is then plunged into liquid ethane at its melting point. The frozen specimen is transferred under liquid nitrogen to the TEM where it is kept at about 45 K in a modified cold stage.[26]

An important modification of this technique has been the addition of a controlled atmosphere chamber to the system that makes it possible to prepare the specimens under controlled humidity (or other volatile saturation) and temperature conditions. This controlled environment vitrification system (CEVS) allows us to quench specimens from any temperature in the 20–90 °C range without change of concentration due to evaporation prior to freezing. It also allows the thinned specimen to relax for an indefinite time before it is plunged into the cryogen. A detailed description of this modified technique and the CEVS is given by Bellare et al.[24,27] and Bellare.[28]

No stain is used in this specimen preparation technique. The good contrast that is demonstrated in the vitrified specimen is phase contrast, a result of proper defocusing of the TEM's objective lens. Defocus values of 1–4 μm ("underfocus") have been used to bring out details on the order of 1–5 nm.[29] Although no gross structural rearrangement is taking place during specimen preparation, big liposomes have been found to be flattened during specimen thinning. Thinning also pushes bigger particles to the hole edges and thus may change the local size distribution of the dispersed aggregates.

Specimens were examined in a JEOL 100CX analytical electron microscope, operating at 100 kV in the conventional TEM mode. The frozen specimens were mounted into a modified JEOL EM-SCH cooling holder using a cold-stage transfer module (CSTM).[26] Images were recorded on Kodak SO-163 film and developed for 12 min in full-strength Kodak D-19 developer.

2.2. Video-Enhanced Microscopy (VEM). There are two major limitations to the use of light microscopy in the characterization of surfactant microstructures. Contrast limitations place a lower bound on the size of aggregate that can be selected for study, while resolution limitations restrict the amount of structural information that can be extracted from microscopic observations.

Many surfactant aggregates, vesicles and microtubules in particular, are of inherently low contrast and cannot be distinguished from the background solution with ordinary light microscopy techniques. While optical methods such as differential interference contrast[30] go a long way in boosting the contrast of such objects, one is still limited by the inability of the eye to

(25) Talmon, Y.; Adrian, M.; Dubochet, J. *J. Microsc. (Oxford)* **1986**, *141*, 375.
(26) Perlov, G.; Talmon, Y.; Falls, A. H. *Ultramicroscopy* **1983**, *11*, 283.
(27) Bellare, J. R.; Davis, H. T.; Scriven, L. E.; Talmon, Y. Paper presented at the 11th International Congress on Electron Microscopy, Kyoto, Sept 1986.
(28) Bellare, J. R. Paper presented at the Proceedings of the 44th Annual Meeting of the Electron Microscopy Society of America, San Francisco, Aug 1986.
(29) Misell, D. L. *Image Analysis, Enhancement and Interpretation*; North-Holland: Amsterdam, 1978; Chapter 3.2.
(30) Allen, R. D.; David, G. B.; Nomarski, G. *Z. Wiss. Mikrosk. Mikrosk. Tech.* **1969**, *69*, 193.

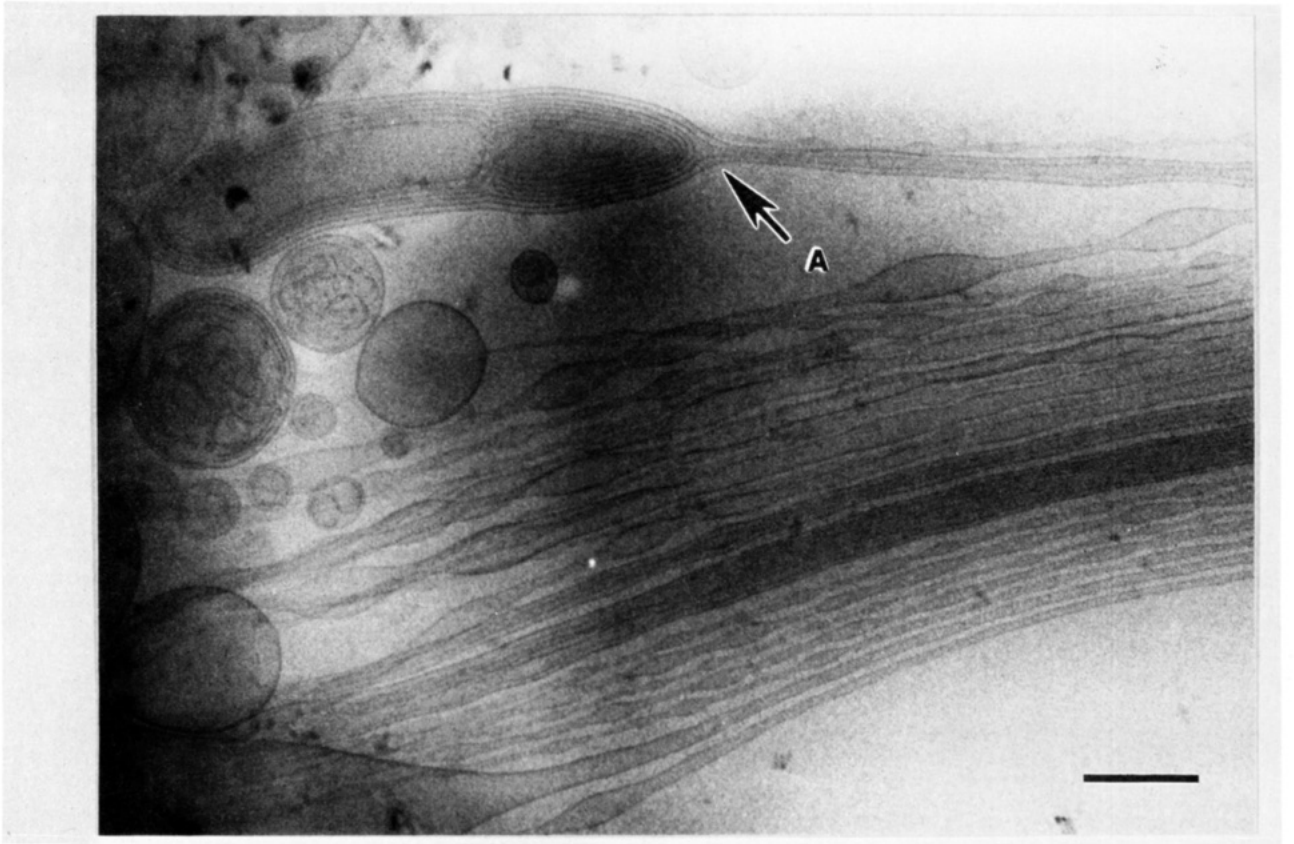

Figure 9. VHU cryo-TEM picture of 1.7 wt % SHBS showing existence of single- and multiple-walled tubules. Note liposome–tubule transition (A). Bar = 0.25 μm.

distinguish small differences in intensity at the high light levels needed for good resolution. This limitation is overcome by using a television camera and a computer capable of real-time digital image processing.

Unlike the human eye, which is a quasi-logarithmic device and saturates at high light levels, a television camera is a linear device; it responds equally well to small differences in intensity no matter what the background light level is. Thus, a television camera linked to a differential interference contrast microscope (VEM)[31-34] improves contrast by responding linearly to contrast at all light levels. Note that the acronym VEDICM[33-36] (for video-enhanced differential interference contrast microscopy) has been shortened here to VEM.

Further contrast enhancement is provided by a computer capable of real-time digital image processing. The computer takes the analog electronic signal from the television camera and converts each $^1/_{30}$-s frame into a 512 × 512 matrix of gray level values ranging from 0 to 255. Since the eye can detect at most 64 shades of gray,[37] the digital image obviously contains more information than the eye can see. The goal of image processing, then, is to take these matrices of gray level values and perform mathematical manipulations on them to extract useful information.[38]

One such manipulation is background subtraction. The contrast intensive technique of linking video with differential interference contrast has an undesirable side effect: inaccessible dirt and lens imperfections create a background mottled pattern that can obscure the objects of interest. If an image of this mottled pattern is stored in computer memory, however, it can be subtracted frame by frame from the actual image. The result is significantly improved image quality.[39]

Another manipulation that is performed by the image processor is the gray-scale transformation or linear stretch. Suppose, for example, that due to a sample of very low contrast (such as small unilamellar vesicles), all the information in an image is contained in the gray-level values between 120 and 140. The eye cannot resolve all 20 of these levels, and much information is lost. By performance of a gray scale transformation, however, all values of gray below 120 can be transformed to black and all values greater than 140 to white with varying shades of gray interpolated between 120 and 140. Thus, the original 20 shades of gray have been expanded into 256 shades.

The discipline of digital image processing allows for other, more complex mathematical transformations. These include various filter operations to enhance edges or eliminate random noise and routines to automatically find all particles of a given contrast threshold and subsequently give statistical information on the size and shape distributions.[38]

As a result of this contrast enhancement, small, isolated colloidal particles like unilamellar vesicles or latex spheres can be detected at a range far lower than that accessible to normal light microscopy. For the present experiment a Nikon Optiphot-Pol microscope fitted with rectified differential interference contrast optics is used. A Dage Model NC68 black and white television camera with a Newvicon imaging tube is interfaced to this microscope by a Nikon 0.9–2.25X zoom lens. Digital image processing is performed by the Psicom 327 system (Perceptive Systems, Houston, TX). With this equipment latex particles of 0.086-μm diameter are clearly visualized. Spheres of 0.06 μm can be detected but only under optimal conditions. The apparent size limitation of the system is therefore between 0.05 and 0.06 μm (50–60 nm).

There is an important distinction between resolution and detection which leads to the second major limitation of light mi-

(31) Inoué, S.; Tilney, L. G. *J. Cell. Biol.* **1982**, *93*, 812.
(32) Allen, R. D.; Allen, N. S.; Travis, J. L. *Cell Motil.* **1981**, *1*, 291.
(33) Kachar, B.; Evans, D. F.; Ninham, B. W. *J. Colloid Interface Sci.* **1984**, *100*, 287.
(34) Evans, D. F.; Brady, J.; Kachar, B.; Ninham, B. W. *J. Solution Chem.* **1985**, *14*, 141.
(35) Brady, J. E.; Evans, D. F.; Kachar, B.; Ninham, B. W. *J. Am. Chem. Soc.* **1984**, *106*, 4279.
(36) Brady, J. E., et al. *J. Phys. Chem.* **1986**, *90*, 1853.
(37) Wechsler, H., private communication.
(38) Castleman, K. R. *Digital Image Processing*; Prentice-Hall: New York, 1979.
(39) Allen, R. D.; Allen, N. S. *J. Microsc. (Oxford)* **1983**, *129*(1), 3.

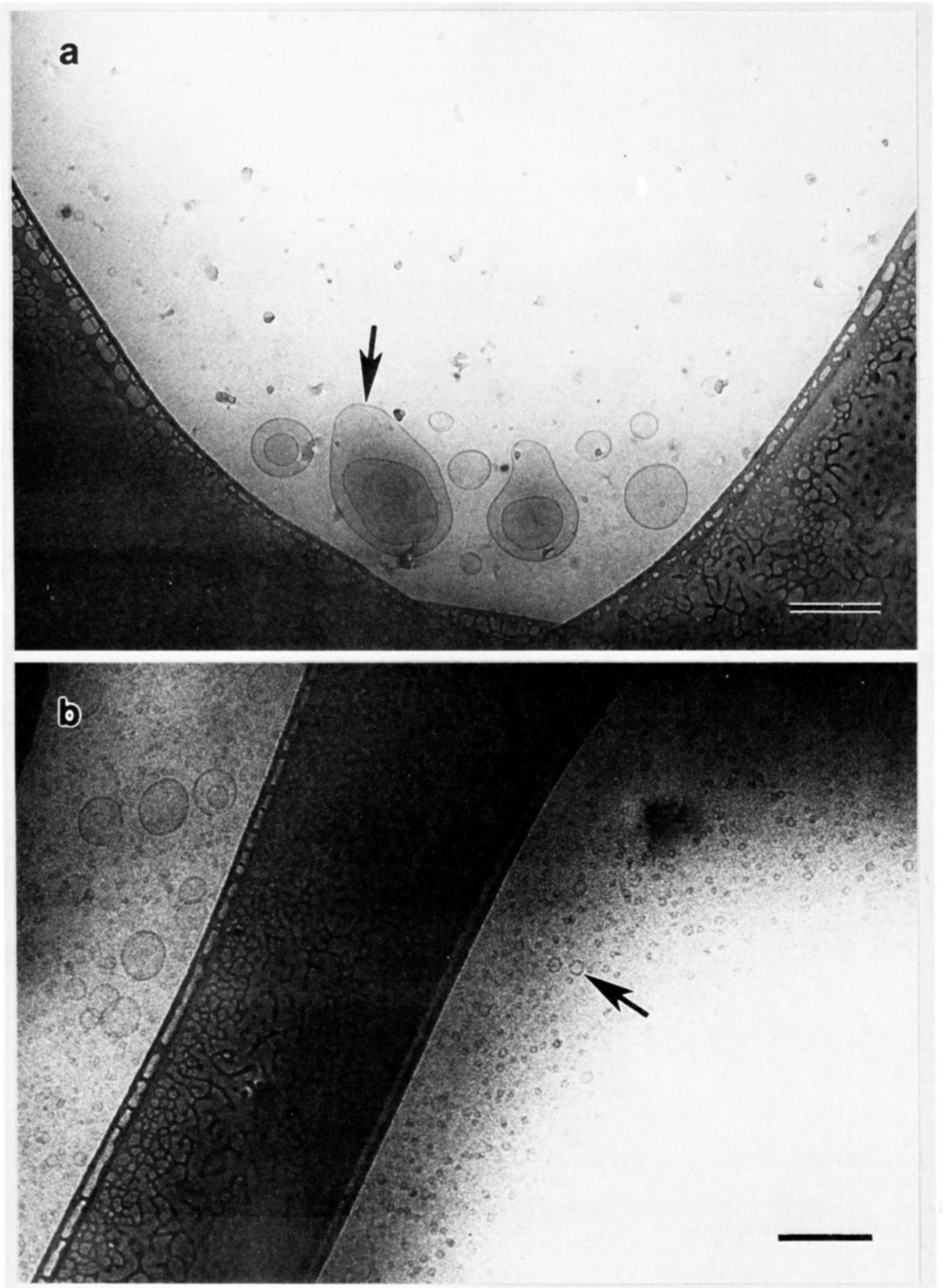

Figure 10. Aqueous dispersions of didodecyldimethylammonium acetate prepared with CEVS and examined with cryo-TEM. Bar = 0.25 μm. (a) Large single- and double-walled vesicles (arrow) at 0.5 wt %; (b) smaller single-walled vesicles at 1.0 wt %.

croscopy. Resolution refers to the ability to distinguish closely spaced objects, but detection simply refers to the ability to observe isolated objects in the field of view. The wave nature of light presents a lower limit to resolution, given approximately by the Rayleigh criterion,[40]

$$Y_R = 0.61\lambda_0/NA \quad (2)$$

where λ_0 is the free-space wavelength of light used to illuminate the specimen (usually 546 nm for interference contrast), and NA is the numerical aperture of the objective used ($Y_R \cong 0.25$ μm for a 100X objective). However, there is no theoretical limit to the size of an isolated particle that can be detected by microscopy (given sufficient contrast to distinguish the particle from the background). Thus, the contrast-enhancing nature of VEM allows very small objects to be detected. Further, the resolution limit of VEM appears to be a factor of 2 smaller than with normal,

(40) Spencer, M. *Fundamentals of Light Microscopy*; Cambridge University Press: New York, 1982.

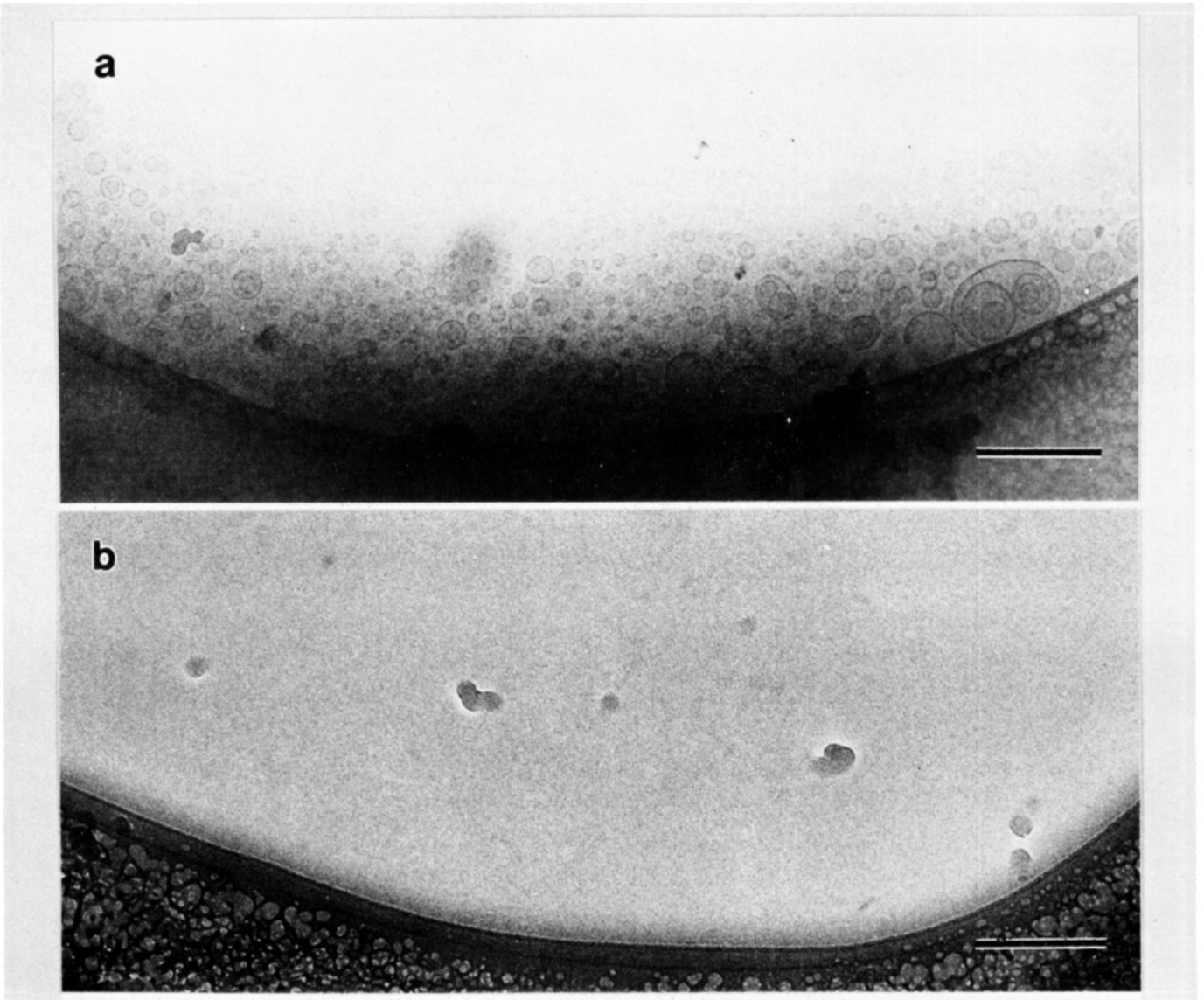

Figure 11. VHU cryo-TEM pictures of aqueous dispersions of SHBS plus the macrocyclic cryptate C222. C222 complexes the Na^+ counterion of SHBS which results in liposomes transforming to vesicles in dilute solutions and micelles in concentrated solution. (a) 0.5 wt % SHBS with a C222-to-surfactant ratio of 0.6. Note unilamellar vesicles with a few multilamellar liposomes. (b) 2% SHBS with a C222-to-surfactant ratio of 1.0. No microstructure is evident. Compare with Figures 6–9. Bar = 0.25 μm.

unaided microscopy. This is because the increased contrast allows a relaxation of the Rayleigh criterion, and the use of a linear detecting device allows the condenser aperture to be opened to its full extent (opening the condenser to its full extent allows more oblique rays to fall upon the specimen and thereby increases resolution; see McCrone[41] and Spencer[40] for more complete explanations of this (Abbe's) theory of resolution) with no loss of contrast due to intensity saturation.

For particles below the resolution limit of the microscope, no accurate size, shape, or other structural information can be obtained. Objects below the resolution limit ($\sim$100 nm for VEM), because of diffraction, appear larger than they are. There is good evidence[31,32,39] that extended structures with one dimension less than 60 nm can be detected. For example, Inoue[31] was able to detect the extension of the acrosomal process in Thyone sperm (diameter = 50 nm), and Allen and Allen[39] detected long microtubule fibers of 10-nm diameter (as evidenced by electron microscopy) by using VEM. Such observations suggest that single bilayers (thickness = 6 nm), if long enough, can be detected by VEM.

Examination of surfactant microstructures with VEM can produce a number of artifacts. Consider what happens when a small drop of sample is placed on a microscope slide and covered with a cover slip. As the sample thins, flexible surfactant aggregates are subjected to shear. For example, if vesicles are attached to the glass surfaces, the shear results in the formation of long filaments connecting the vesicle to the glass surfaces (Figure 6, ref 33). When the flow stops, the vesicles travel back up the filament and reattach to the glass. Another problem results from solvent evaporation which can lead to convection and osmotic strain. For dipalmitoylphosphatidylcholine–cholesterol liposomes[42] and didodecyldimethylammonium carboxylate vesicles, evaporation induces a transformation to wormlike structures. Evaporation effects can be retarded by sealing the edges of the cover slip with a blend of purified paraffins and polymers.

Shearing and evaporation artifacts can be minimized by constructing sample cells with 1-mil (0.001 in. $\cong$ 0.025 mm) thin metal annular spacers glued onto the microscope slide. In constructing such cells, the following limitation must be kept in mind. At high levels of magnification (100X objective), the total working distance between the condenser and objective is 2 mm, and one is constrained to cover slips of 0.17 $\pm$ 0.01 mm thickness for optimal resolution and contrast.[43]

In order to utilize the ability of VEM to follow chemically

(41) McCrone, W. C.; McCrone, L. B.; Delly, J. G. *Polarized Light Microscopy*; McCrone Research Institute: New York, 1984.

(42) Hotani, H. *J. Mol. Biol.* **1984**, *178*, 113.

(43) Spinell, B. M.; Loveland, R. P. *J. Royal Microsc. Soc.* **1960**, *79*(1), 59.

induced transformations, control of flow and reagent concentrations is required. A crude approach is to mix a solution (e.g., didodecyldimethylammonium hydroxide vesicles) contained between cover slip and slide and a drop of reagent (e.g., HBr) by drawing the reagent into the solution with tissue paper. This results in uncontrolled convection and the formation of large liposomes (Figure 2).

These same transformations can be carried out in a controlled manner by using the flow cell devised by Miller et al.[44] The cell consists of two stainless steel plates separated by a thin (0.025–0.075 mm) Teflon or rubber gasket. The plates have rectangular slots into which a microscope slide (for the bottom plate) and a cover slip (for the top plate) can be secured with an optical adhesive. The top plate has three entrance ports at one end and an exit port at the other end. For simple flow experiments, fluid is fed into the middle port and flows down a single slot cut in the gasket. When the flow is stopped, the relaxation of surfactant microstructures back to their unperturbed form can be followed. With a T-tube mixer attached to the inlet, the cell can be used for stopped-flow microscopy.

Alternately, solution and reagent can be pumped into the two outside ports and allowed to flow down the gasket with a Y-shaped groove (Figure 3). The two impinging streams form a sharply defined steady-state interface. When the flow is stopped, controlled mixing occurs across the interface and can be followed on video tape. Such a sequence is shown for the neutralization of didodecyldimethylammonium hydroxide ($2C_{12}N2C_1OH$) with HBr (Figure 4).

3. Comparison of Cryo-TEM and VEM

With the advantages and limitations of the two techniques in mind, we now demonstrate their usefulness and complementarity. Pictures by themselves are meaningless unless we have some idea of what the picture represents. The one firm unifying notion we have is that microstructure—the size and shape of aggregates—must be systematically related to curvature. And curvature must be related to molecular properties which prescribe head group and interaggregate interactions. We choose two surfactant systems which illustrate this interplay. These are an anionic double-chained surfactant SHBS (sodium 8-phenyl-*n*-hexadecyl-*p*-sulfonate or Texas No. 1) and cationic dialkyldimethylammonium hydroxide, acetate, and bromides.

3.1. SHBS—A Diversity of Structures. A VEM picture of a 6-month-old, 1.7 wt % SHBS sample (Figure 5) shows the existence of polydisperse liquid crystalline aggregates with a wide diversity of stuctures. The large structures (points A and B, Figure 5) show birefringence and the Maltese crosses characteristic of liquid crystalline liposomes[45] when the VEM optics are switched to polarizing optics without moving the microscope slide. The undulations of individual layers within the birefringent liposomes (point B, Figure 5) and the caged movement of smaller vesicles entrapped within larger vesicles (point C, Figure 5) can be followed in real time. Of particular interest is the "unstructured" spherical region of diameter $\approx 9\ \mu$ (point D, Figure 5), which in real time shows a "sand storm" appearance associated with very small structures. A large number of other small structures which are beyond the resolution limit of the light microscope are also evident.

The cryo-TEM pictures of the same 1.7 wt % SHBS sample (Figures 6–9) reveal the coexistence of vesicles within vesicles (Figure 6), coiled tubules within vesicles (Figure 7), and liposomes (Figure 8) in which bilayer walls are visible in the clear field produced by vitrified ice: particularly interesting is Figure 7, in which incorporated inside the core of the larger vesicles is an astonishing menagerie of coiled tubules, smaller vesicles, and beaded tubes which appear to have been frozen in the process of transforming to small unilamellar vesicles. These intricate structures do not appear to be artifacts associated with sample preparation since the same structures are obtained when the thinned samples are held in the environmental chamber for 30 min before plunging into liquid ethane. Note that the large birefringent liposomal structures (<5 μm) evident by polarizing microscopy and VEM are absent and probably located in the regions of the vitrified ice that are too thick for viewing.

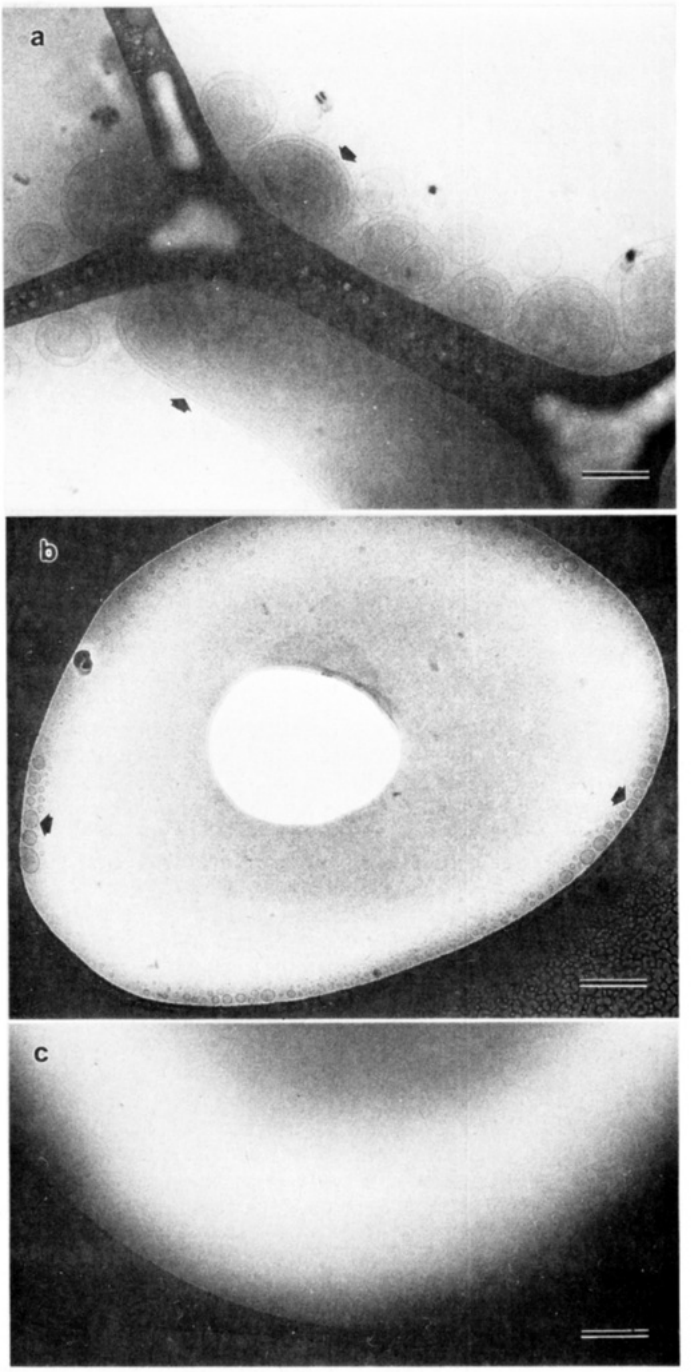

Figure 12. Didodecyldimethylammonium bromide prepared at 25 and 70 °C with CEVS: (a) 25 °C and 1.5 wt % showing large liposomes; (b) 70 °C and 0.4 wt % showing the transformation to vesicles in dilute solution; and (c) 70 °C and 1.5 wt % giving a clear field with no visible aggregates. Whether the graininess in this electron micrograph represents micelles or noise is unresolved. Bar = 0.25 μm.

Of particular interest for the comparison of cryo-TEM and VEM is the enclosed vesicle structure (point A, Figure 6) of diameter 1.75 μm which contains a large number of small unilamellar vesicles. We believe that this structure is similar to the VEM structure of point D, Figure 5. In fact, the sequence of structures point C, Figure 5 ($D \simeq 15\ \mu$m); point D, Figure 5 ($D = 9\ \mu$m); point A, Figure 6 ($D = 1.75\ \mu$m); and point B, Figure 8 ($D = 0.01\ \mu$m) suggests that cryo-TEM and VEM visualize a continuity of self-similar structures (i.e., structures of similar

(44) Miller, D. D.; Evans, D. F.; Brady, J. E. Paper presented at the National Meeting of the AIChE, Chicago, Nov 1985.
(45) Franses, E. I., et al. *J. Phys. Chem.* **1980**, *84*, 1547.

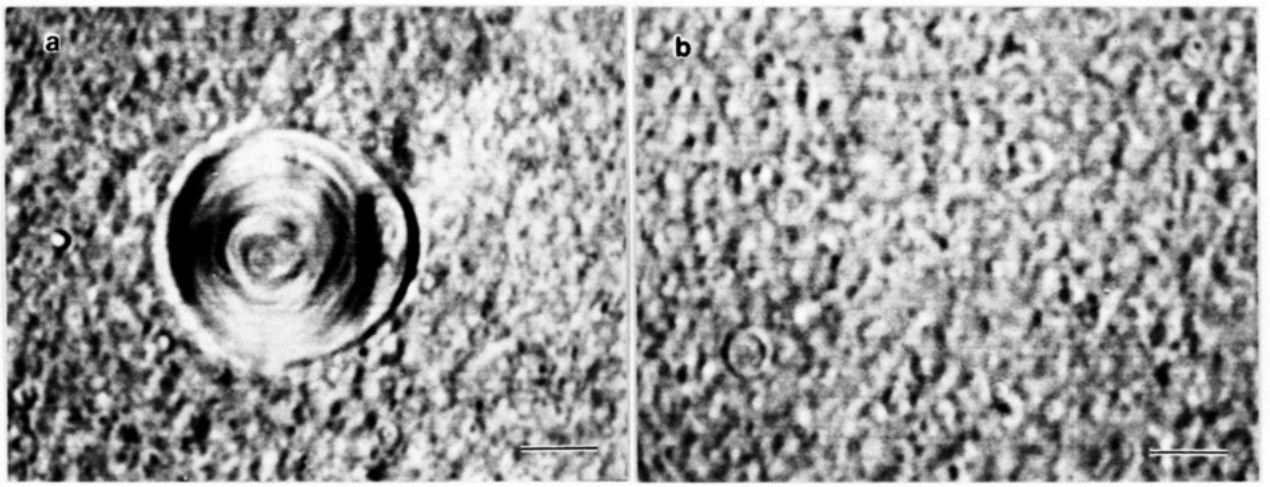

Figure 13. Didecyldimethylammonium bromide at 25 °C by VEM. Bar length = 5 μm. (a) 1.5 wt %—note the large liposome (birefringent under crossed polars) immersed in a sea of smaller particles. The Maltese cross visible in liquid crystalline liposomes viewed under crossed polars can also be seen, though faintly, here (note the dark regions on the "east" and "west" portions of the liposome). DIC optics can produce Maltese crosses in strongly birefringent liposomes since crossed polars are used with this technique. (b) 0.4 wt %—many particles are resolved but there are few large liposomes. By comparison, at 70 °C, the 1.5% solution shows no structures by VEM, while the 0.4% solution contains only small vesicles that are visible but below the resolution limit of VEM.

topology but different sizes). We return to these structures later.

The collection of microtubules displayed in Figure 9 demonstrate the existence of both single-walled and multiwalled microtubules. The multimicrotubules attached to the liposome structure (point A, Figure 9) are reminiscent of larger but similar vesicle–filament structures seen by VEM with didodecyldimethylammonium hydroxide partially neutralized by HBr.[33]

The preceding observations allow some important conclusions to be drawn regarding the use of cryo-TEM and VEM. While cryo-TEM, because of its much higher resolving power, is clearly the technique of choice when detailed structural information is desired, it cannot be used exclusively to characterize a given sample. This is because the sample preparation procedure seems to cause a sorting of aggregates based on size. The result is that aggregates of certain sizes are overrepresented in TEM pictures, while other aggregates are excluded (recall that the large birefringent liposomes seen with VEM are absent in the TEM micrographs). Since VEM images all structures from 50 nm to 500 μm, it is used to initially characterize a solution in terms of size, type, and relative number of aggregates present. Subsequent detailed structural information on these aggregates can be achieved by using cryo-TEM.

Another example of the use of both techniques is illustrated below.

3.2. Microstructures in Isotropic Phases—Vesicles and Micelles. Didodecyldimethylammonium hydroxide and carboxylates form clear nonviscous solutions up to 0.5 M.[46] In dilute solutions (10^{-3}–10^{-2} M), only small particles beyond the resolution limit are detected by VEM. Examination of $2C_{12}N2C_1OAc$ by cryo-TEM establishes the presence of vesicles (Figure 10a) which decrease in size upon concentration (Figure 10b). Above 0.1 M, both cryo-TEM and VEM give pictures devoid of any structure.

The decreasing size of the vesicle structure with concentration for $2C_{12}N2C_1OAc$ constitutes a direct visualization of the conclusions drawn from fluorescence measurements.[36] These conclusions were that the fraction of surfactant present as vesicles in the solution decrease from ~0.99 at 10^{-3} M to ~0 at 10^{-1} M and that the micelles were small (aggregation number 45) and remained of constant size across the vesicle–micelle transition range. This behavior can be rationalized by direct force measurements between bilayers[8,10] which link head group forces directly to curvature and microstructure.

In an attempt to emphasize the dynamic behavior of these systems as seen by VEM, we show four pictures (Figure 4) from a 60-min sequence of the neutralization of 10^{-3} M $2C_{12}N2C_1OH$ with 10^{-3} M HBr in the flow cell. The direction of flow is from left to right, and the surfactant solution is in the bottom half of the picture. When the flow is stopped, the vesicles near the interface grow upon neutralization. Small wormlike structures become visible. They increase in length and begin to form larger vesicle and liposome structures. After 1 h, the worms have also completely disappeared. A similar sequence (not shown) starting with a 0.01 M micellar solution proceeds much more rapidly, and the worms are much less evident. Neutralization by free convection (Figure 2) yields much larger structures. The transformation occurs with an almost explosive-like violence. It is worth reiterating that the sequence of events as summarized by still pictures provides a poor substitute for the dynamics as revealed by video.

The same vesicle–micelle transformation with increasing surfactant concentration can also be induced in SHBS by addition of the cryptate C222.[46] This macrocyclic compound forms large inclusion complexes with the sodium counterion, thereby pulling it out from amongst the surfactant head group. The resulting electrostatic repulsion drives the head groups apart and induces more curvature which favors smaller aggregates.[47] For a 0.5% SHBS solution containing C222, only small vesicles are visible (Figure 11a). For a 2.0% SHBS solution with C222 (Figure 11b) the electron microscope picture is devoid of any structure (it is impossible to decide where the residual graininess is micelles or noise). For comparison purposes (~2%) SHBS without C222 is shown in Figures 6–9.

3.3. High-Temperature Systems. The chemical systems which display vesicle–micelle transitions described above involve unusual counterions (OH^-, OAc^-) or complexing agents. This can be understood in terms of a primitive model theory if these counterions behave as large "hydrated" hard core spheres. Of more interest to our main theme is a system employing didecyldimethylammonium bromide ($2C_{10}N2C_1Br$) with the more familiar bromide counterion. At elevated temperatures, this system forms a clear isotropic "micellar" phase. Its microstructure, which has not been previously explored, varies continuously within a single-phase region and surprisingly shows the same vesicle-to-micelle transition as the unusual counterions at lower temperatures. Thus, if dilute $2C_{10}N2C_1Br$ is heated to 70 °C in the CEVS chamber and then plunged into liquid ethane, small vesicular structures (Figure 12b) are seen. Upon concentration, only clear fields are seen in cryo-TEM pictures (Figure 12c). Parallel to this, with VEM at 70 °C very small structures are observed in dilute solution, no structures in concentrated solution. For comparison cryo-TEM

(46) Miller, D. D.; Evans, D. F.; Warr, G. G.; Bellare, J. R.; Ninham, B. W. *J. Colloid Interface Sci.*, in press.

(47) Mitchell, D. J.; Ninham, B. W. *J. Chem. Soc., Faraday Trans. 2* **1981**, *77*, 601.

(Figure 12a) and VEM (Figure 13) micrographs of $2C_{10}N2C_1Br$ at 25 °C show multiwalled vesicles and liposomes. Fluorescence-probe quenching experiments (to be detailed elsewhere)[48] on this system at 70 °C are consistent with the cryo-TEM and VEM results. These observations provide a challenge to existing theories which can account for these phenomena only if postulated hard core size depends on temperature. The power brought to bear by parallel use of these techniques is evident.

4. Discussion

The apparent existence of self-similarity is of some importance. Models of surfactant aggregation used for interpretation of the structure by other techniques are of two kinds. The first postulates regular arrays like hexagonal, cubic, or lamellar phase from which scattering form factors are calculated and fitted to experiment. The second utilizes low level statistical mechanical theories which treat interactions as a perturbation. These latter have the virtue that they relate optimal equilibrium aggregates to molecular geometry and interactions. But they are limited because we have no idea of how to write down a partition function which simultaneously averages over shapes and energies. Neither approach, therefore, can easily accommodate the kind of self-similar microstructures seen here. Nonetheless, there are clues which suggest that self-similarity can be a quite general phenomenon. Thus, an assumed vesicle size[47] is determined by a delicate interplay between outer surfactant curvature (head group vs. tail forces) as measured by the surfactant parameter v/al (where v is the volume occupied by the hydrophobic chain(s), a is the area occupied per hydrophilic head group, and l is the effective length of the hydrophobic chain(s)), intervesicle forces which perturb that interaction, and internal layer chain packing constants. At the surfactant–water interface, the balance of forces leads to a zero or very low tension. Curvature energies are low. Hence, if the chains are sufficiently flexible, there is no reason not to admit microtubules, or undulating structures into the scheme of things. For ionic surfactants in topologically closed aggregates, inside and outside counterion concentrations are very different because of the requirements of electroneutrality. Hence, surfactants inside an aggregate see a different microenvironment to those outside, and those inside can sometimes assemble into smaller closed structures within which can be still smaller structures until the limiting micellar length scale is reached.

(48) Miller, D. D.; Warr, G. G.; Evans, D. F.; Ninham, B. W., unpublished results.

Godel's theorem tells us that within any axiomatic system of logic there are acceptable propositions, the truth of which cannot be decided. The situation that faces physical chemistry in its attempt to join association chemistry to cell biology through membrane mimetic systems is in some ways reminiscent of that which faced mathematics last century. Realization that the proposition that two parallel lines will not meet at a point was indeed a separate Euclidean axiom led to non-Elucidean geometries that really do apply to the world. And Hamilton's discovery of quaternions led to the further realization that there are not one but many algebras. While not precisely axioms, the assumptions involved necessary to characterize surfactant assemblies with noninvasive techniques have tended to take on the status of axioms. Characterization in terms of an assumed (mathematically tractable) limited class of structures provides a self-fulfilling interpretation which cannot easily reveal the enormously rich microstructure shown by surfactant aggregates. This microstructure is directly connected to those hidden molecular parameters which prescribe shape and size and variations thereof. The new techniques we have illustrated are themselves limited and are not necessarily artifact free. Nonetheless these techniques do display the systematic operation and interplay between variables like counterion type, counterion antagonism, chain length, temperature, and concentration, which directly relates to curvature through measurable molecular forces. They also show up the extraordinary range of microstructures that exist within a single phase. Further the diversity of structures revealed demands that any statistical mechanical description which links molecular to aggregate properties must eventually call on a geometric topology to be even an approximate representation of reality. In mathematics itself, the notion of a proof is now conceded to be intuitive and a matter of convention. So too that previous certitude in explaining amphiphilic systems which derived from confidence in assigning a meaning to phases has to be tempered. That is hardly a matter for dismay, because a broadening of the kinds of structures allowed by current theory adds a new and richer dimension better connected to reality.

Acknowledgment. D.D.M. acknowledges funding from the National Science Foundation. D.D.M. and D.F.E. thank J. M. Oakley for the flow cell drawing. J.R.B. thanks his advisors, Profs. L. E. Scriven and H. T. Davis. This work was funded by U.S. Army Grant DAAG29-85-K-0169, NIH Grant IROI-Gm 34341-01, NSF equipment Grant NSF/CPE-8312539, and NSF Grant NSF/CPE-8215342.